The PDZ Protein Mupp1 Promotes G i Coupling and Signaling of the Mt 1 Melatonin Receptor

Jean-Luc Guillaume, Avais M Daulat, Pascal Maurice, Angélique Levoye, Martine Migaud, Lena Brydon, Benoit Malpaux, Catherine Borg-Capra, Ralf Jockers

THE JOURNAL OF BIOLOGICAL CHEMISTRY VOL. 283, NO. 24, pp. 16762–16771, June 13, 2008

The PDZ Protein Mupp1 Promotes G_i Coupling and Signaling of the Mt_1 Melatonin Receptor*[S]

Received for publication, March 14, 2008 Published, JBC Papers in Press, March 31, 2008, DOI 10.1074/jbc.M802069200

Jean-Luc Guillaume[‡§], Avais M. Daulat[‡§1], Pascal Maurice[‡§], Angélique Levoye[‡§2], Martine Migaud[¶], Lena Brydon[‡§3], Benoît Malpaux[¶], Catherine Borg-Capra[‖], and Ralf Jockers[‡§4]

From the [‡]Institut Cochin, Department of Cell Biology, Université Paris Descartes, CNRS (UMR8104), Paris 75014, France, [§]Inserm U567, Paris 75014, France, [¶]Physiologie de la Reproduction et des Comportements, UMR 6175 INRA-CNRS-Université François Rabelais de Tours-Haras Nationaux, Nouzilly 37380, France, and [‖]Hybrigenics, Paris 75014, France

Intracellular signaling events are often organized around PDZ (PSD-95/*Drosophila* Disc large/ZO-1 homology) domain-containing scaffolding proteins. The ubiquitously expressed multi-PDZ protein MUPP1, which is composed of 13 PDZ domains, has been shown to interact with multiple viral and cellular proteins and to play important roles in receptor targeting and trafficking. In this study, we show that MUPP1 binds to the G protein-coupled MT_1 melatonin receptor and directly regulates its G_i-dependent signal transduction. Structural determinants involved in this interaction are the PDZ10 domain of MUPP1 and the valine of the canonical class III PDZ domain binding motif DSV of the MT_1 carboxyl terminus. This high affinity interaction ($K_d \sim 4$ nM), which is independent of MT_1 activation, occurs in the ovine pars tuberalis of the pituitary expressing both proteins endogenously. Although the disruption of the MT_1/MUPP1 interaction has no effect on the subcellular localization, trafficking, or degradation of MT_1, it destabilizes the interaction between MT_1 and G_i and abolishes G_i-mediated signaling of MT_1. Our findings highlight a previously unappreciated role of PDZ proteins in promoting G protein coupling to receptors.

The concept of organized networks has emerged in the field of cellular signaling in the last few years. Assembling the different partners in close proximity optimizes the spatial and temporal organization and the specificity of the cellular response. The assembly of these multimolecular complexes occurs through the interaction of modular domains recognizing their target counterparts. PDZ domains are widely spread modules exhibiting this function. Data bank exploration with SMART (1) identifies 584 PDZ domains in 328 different proteins in the human genome.

G protein-coupled receptors (GPCRs)[5] constitute the largest family of membrane receptors, and many of the more than 750 members have been shown to interact with PDZ domain-containing proteins, either constitutively or upon agonist activation (2). Binding of PDZ proteins to GPCRs has been reported to primarily regulate subcellular localization, trafficking, and stability of receptors (3). For instance, binding of MUPP1 and syntrophins to the γ-aminobutyric acid type B ($GABA_B$) receptor and the α_{1D}-adrenergic receptor, respectively, significantly increases receptor stability (4, 5). In other cases, PDZ scaffolds determine the subcellular localization of GPCRs (6) and receptor endocytosis as shown for PSD-95 and the 5-HT_{2A} serotonin and β_1-adrenergic receptors (7, 8). PDZ proteins, such as NHERF and hScrib, are also important for the recycling of receptors to the cell surface (9–11).

Binding of PDZ proteins to GPCRs also modulates receptor signaling by assembling proteins involved in signal transduction. NHERF family proteins are known to regulate the activity of the Na^+/H^+ exchanger through association with NHERF-1 (12) and to form a ternary complex with phospholipase Cβ3 and GPCRs, which enhances the signaling efficiency of the receptor-mediated activation of the phospholipase $C\beta/Ca^{2+}$ pathway (13–15). Binding of GIPC (GAIP-interacting protein, COOH terminus) to the COOH terminus of the D3 dopamine and the β_1-adrenergic receptor (16) decreased $G\alpha_i$-mediated signaling of these receptors most likely through RGS19, which binds to GIPC (17). Further examples of PDZ scaffolds that regulate GPCR signaling include a ternary complex formation around the PDZ scaffold MAGI-3, which binds to the GPCR frizzled-4 and Ltap to regulate the JNK signaling cascade (18), as well as PDZ-domain-containing Rho guanine nucleotide exchange factors that interact with lysophosphatidic acid 1 and 2 receptors to activate RhoA (19).

To identify proteins that specifically interact with the G protein-coupled human MT_1 and MT_2 melatonin receptors, we

* This work was supported by grants from Hybrigenics, the Institut de Recherches SERVIER, the Fondation pour la Recherche Médicale (Equipe FRM), and the Fédération pour la Recherche sur le Cerveau/FRC Neurodon. The costs of publication of this article were defrayed in part by the payment of page charges. This article must therefore be hereby marked "*advertisement*" in accordance with 18 U.S.C. Section 1734 solely to indicate this fact.

[S] The on-line version of this article (available at http://www.jbc.org) contains supplemental Fig. S1.

[1] Recipient of an EGIDE fellowship.

[2] Present address: Institut Pasteur, Laboratoire de Pathogénie Virale Moléculaire, Inserm U819, Dépt. de Virologie, 28 Rue du Dr. Roux, 75724 Paris, France.

[3] Present address: University College and Royal Free Medical School, Department of Epidemiology and Public Health, Psychobiology Group, London WC1E 6BT, United Kingdom.

[4] To whom correspondence should be addressed: Institut Cochin, 22 Rue Méchain, 75014 Paris. Tel.: 331-40-51-64-34; Fax: 331-40-51-64-30; E-mail: jockers@cochin.inserm.fr.

[5] The abbreviations used are: GPCR, G protein-coupled receptor; $GABA_B$, γ-aminobutyric acid type B; 5-HT, 5-hydroxytryptamine; C-tail, carboxyl-terminal tail; PT, pars tuberalis; CHAPS, 3-[(3-cholamidopropyl)dimethylammonio]-1-propanesulfonic acid; BRET, bioluminescence resonance energy transfer; siRNA, small interfering RNA; ERK, extracellular signal-regulated kinase; MLT, melatonin; AC, adenylyl cyclase; PTX, pertussis toxin; HA, hemagglutinin; GST, glutathione *S*-transferase.

performed a yeast two-hybrid screen using the cytoplasmic domains of these receptors as baits. The multi-PDZ domain protein MUPP1 was identified as interacting partner of the carboxyl-terminal tail (C-tail) of MT_1 but not of MT_2. Importantly, this interaction was necessary for the stabilization of the MT_1-G_i complex and efficient G_i-dependent signaling of MT_1.

EXPERIMENTAL PROCEDURES

Yeast Two-hybrid Screen—The cDNA sequences corresponding to the intracellular loops i2 (residues 123–141), i3 (residues 208–239), and the C-tail (residues 294–350) of MT_1 or the C-tail alone were inserted in frame in the pB6 yeast expression vector derived from the original pAS2ΔΔ (20). A random-primed, size-selected (mean insert size 800 bp) cDNA library of differentiated human brown adipocyte PAZ6 cells (21) was constructed in the pB6 vector derived from the original pGADGH vector. Plasmids able to rescue yeast growth were amplified by PCR and sequenced at their 5′ and 3′ junctions on a PE3700 sequencer. The resulting sequences were used to identify the corresponding interactors in the GenBank™ data base (NCBI) using a fully automated procedure.

Plasmid Constructions and Cell Culture—The GW1-HA-MUPP1 plasmid containing the coding region of the rat MUPP1 as well as GST fusion constructs expressing PDZ1–3, PDZ4-5, PDZ6, PDZ7, or PDZ8-9 were a gift from Dr. Javier and have been described elsewhere (22, 23). GST fusion constructs containing PDZ9, PDZ10, or PDZ11-12 were a gift from Dr. Mancini (24). GST constructs were expressed in *Escherichia coli* and purified on immobilized glutathione according to standard protocols. The FLAG-tagged MT_1 receptor has been described elsewhere (25). Mutants of the MT_1 PDZ binding motif were generated by PCR. Human CCR5 and human SSTR2 somatostatin receptor expression vectors were generously given by Drs. Marullo (Paris, France) (26) and Bousquet (Toulouse, France) (27), respectively. HEK 293 cells were grown and transfected as described (25).

Solubilization and Immunoprecipitation—Cells were lysed for 4 h on ice in lysis buffer (25 mM Hepes, 150 mM NaCl, 2 mM EDTA, 15 mM β-glycerophosphate, 2 mM Na_3VO_4, 10 mM NaF, 5 μg/ml leupeptin, 10 μg/ml pepstatin, 10 μg/ml benzamidine, 1 mM 4-(2-aminoethyl)-benzenesulfonyl fluoride) containing 1% Nonidet P-40, 0.5% deoxycholate, and 0.1% SDS, and lysates were centrifuged at 26,000 × *g* for 30 min at 4 °C. Receptor immunoprecipitation was done on supernatant by the anti-FLAG M2 antibody (Sigma) preadsorbed on Protein G. Immunoadsorbed material was pelleted by centrifugation, submitted to SDS-PAGE, and transferred to nitrocellulose. Immunoblot analysis was carried out with the polyclonal anti-MUPP1 antiserum at 1:20,000 dilution (a gift from Dr. Javier) (22, 23) or the polyclonal anti-FLAG antibody (Sigma), and immunoreactivity was revealed using a goat anti-rabbit secondary antibody coupled to horseradish peroxidase and the ECL chemiluminescent reagent (Amersham Biosciences).

Ovine pituitary pars tuberalis (PT) were collected, and crude membranes were prepared as described previously (28). Radioligand binding was performed with PT membranes (1.5–2 mg of protein) in 1 ml of TEM buffer (75 mM Tris, 12 mM $MgCl_2$, 2 mM EDTA, protease inhibitor mixture EDTA-free, pH 7.4), using 400 pM [2-^{125}I]iodomelatonin ([^{125}I]MLT) (PerkinElmer Life Sciences) for 90 min at 37 °C. After membrane solubilization with 1% digitonin (overnight, 4 °C) and centrifugation (90 min, 18,000 × *g*, 4 °C), MUPP1 was immunoprecipitated from solubilized proteins using a combination of 4 μg of monoclonal anti-MUPP1 antibody (BD Biosciences) and 5 μl of polyclonal anti-MUPP1 antibodies preadsorbed on protein G-Sepharose beads. Beads were washed, and immunoprecipitated radioactivity was collected by rapid filtration through glass fiber filters.

G protein co-immunoprecipitation was carried out as described (29). Anti-$G\alpha_q$ (sc-393; Santa Cruz Biotechnology, Inc., Santa Cruz, CA) or anti-$G\alpha_{i3}$ (sc-262; Santa Cruz Biotechnology) was used for Western blotting.

Peptide Affinity Chromatography—Synthetic peptides corresponding to the C-tail of MT_1 (residues 294–350) or MT_2 (residues 305–364) tagged with His_6 were provided by Servier (Suresnes, France). Brains harvested from C57BL6 mice were washed in phosphate-buffered saline; crushed in solubilization buffer composed of 20 mM NaH_2PO_4, 10 mM CHAPS, 150 mM NaCl, 2 mM Na_3VO_4, 10 mM NaF, protease inhibitor mixture EDTA-free (Roche Diagnostics, Meylan, France), pH 8; and incubated for 2 h at 4 °C. The homogenates were centrifuged at 10,000 × *g* (1 h, 4 °C), the supernatants were collected, and 10 mg of solubilized brain proteins were incubated overnight at 4 °C with 20 μl of Ni^{2+}-nitrilotriacetic acid beads (Qiagen, Courtaboeuf, France) coated with His_6-tagged MT_1 or MT_2 COOH-terminal peptides (300–350 μg), in the presence of 20 mM imidazole to reduce nonspecific binding. Bound proteins were eluted by 2% SDS, separated by SDS-PAGE, and checked by Western blotting for the presence of MUPP1 using anti-MUPP1 antibodies.

Immunofluorescence—HEK293 cells stably expressing the FLAG-MT_1 receptor and transfected by HA-MUPP1 DNA were fixed in phosphate-buffered saline containing 4% paraformaldehyde and 0.2% Triton X-100 for 30 min. Monoclonal anti-FLAG M2 antibody and polyclonal anti-HA antibody HA.11 (BAbCo, Richmond, CA) were applied, followed by rhodamine-tagged anti-mouse and fluorescein isothiocyanate-tagged anti-rabbit antibodies. Cells were examined by confocal fluorescence microscopy.

ELISA—The ELISA was adapted from Stricker *et al.* (30). Lysates from *E. coli* expressing different MUPP1 regions fused to GST were coated on ELISA plates. The amount of lysate used for coating corresponded to 50 μl of a 0.1 M $NaHCO_3$ solution, pH 9.5, containing a 20 μg/ml concentration of the fusion protein (as evaluated by Coomassie Blue staining of SDS-PAGE-separated lysate proteins). HEK293 cells transfected by the different FLAG-tagged receptor plasmids were lysed, and 50 μl of lysate were added to the wells for a 3-h incubation at room temperature. ELISA was carried out with anti-FLAG M2 antibody (2 μg/ml), followed by horseradish peroxidase-coupled anti-mouse antibody. Staining was performed with 2-2′-azinobis(3-ethylbenzthiazoline-6-sulfonic acid), and the color intensity was measured at 450 nm.

To determine the affinity of the receptor/PDZ interaction, 50 μl of 0.1 M $NaHCO_3$, pH 9.5, buffer containing 2 μg/ml GST fusion proteins were adsorbed on ELISA plates. The amount of receptor was quantified by [^{125}I]MLT binding, and then the

cells were lysed, and the solubilized receptor concentration was adjusted to 5 nM. Dilutions of the solubilized receptor were incubated on preadsorbed GST-fused PDZ domains, and the ELISA was performed as described above.

Binding Assays—[^{125}I]MLT (PerkinElmer Life Sciences) binding assays were performed on membranes as described (29).

Receptor Internalization—For constitutive internalization, suspended HEK-FLAG-MT_1 cells were incubated with anti-FLAG M2 antibody (1 h, 4 °C). Aliquots were then incubated at 37 °C for variable times. Cells were then transferred to ice, incubated with fluorescein isothiocyanate-coupled secondary antibody, and fixed with paraformaldehyde. The fluorescence was measured by fluorescence-activated cell sorting.

For agonist-stimulated internalization, cells in 6-well plates were incubated in culture medium containing 0.1 μM MLT for variable times (0.5–3 h) and then transferred to ice. Cells were suspended and incubated with anti-FLAG M2 antibody, followed by fluorescein isothiocyanate-coupled secondary antibody to label surface receptor. Fluorescence was measured by fluorescence-activated cell sorting after fixation with paraformaldehyde.

Receptor Degradation—HEK-FLAG-MT_1 cells were plated in polylysine-coated 24-well plates. The next day, protein synthesis was inhibited by treatment for 45 min with 100 μM cycloheximide. Incubation was continued for 4 h in the presence or absence of agonist (0.1 μM MLT). Cells were transferred to ice, fixed, and permeabilized by treatment with cold ethanol at −20 °C for 10 min. ELISAs were performed as described above.

cAMP Assay—Cyclic AMP levels were determined by HTRF using the Cisbio "cAMP femto2" kit according to the manufacturer's instructions. Samples were analyzed with a PheraStar apparatus (BGM Labtech, Offenburg, Germany).

Bioluminescence Resonance Energy Transfer (BRET) Assay, Luminescence, and Fluorescence Measurements—BRET experiments, luminescence, and fluorescence measurements were performed as described on adherent cells (25).

siRNA Treatment—siRNAs corresponding to region 955–973 of the human MUPP1 cDNA were synthesized (Eurogentech, Seraing, Belgium) and transfected with Lipofectamine 2000 (Roche Applied Science) according to the supplier's instructions. Negative control siRNA Alexa Fluor 488 was from Qiagen (catalog number 1022563).

Mitogen-activated Protein Kinase Activation—Activated ERK1/2 were detected by anti-phospho-ERK antibody (sc-7383; Santa Cruz Biotechnology). Levels of loaded proteins were compared by detection of ERK2 (sc-154; Santa Cruz Biotechnology).

Statistical Analysis—Results were analyzed by PRISM (GraphPad Software Inc., San Diego, CA). Data are expressed as mean ± S.E. Student's *t* test was applied for statistical analysis.

RESULTS

The C-tail of MT_1 Specifically Interacts with MUPP1—To identify interacting partners of the human melatonin MT_1 and MT_2 receptors, we conducted yeast two-hybrid screens using the C-tails or a fusion of the intracytoplasmic loops i2 and i3 and the C-tail of these receptors as baits (Fig. 1*A*). The screens were performed against a cDNA library of differentiated human

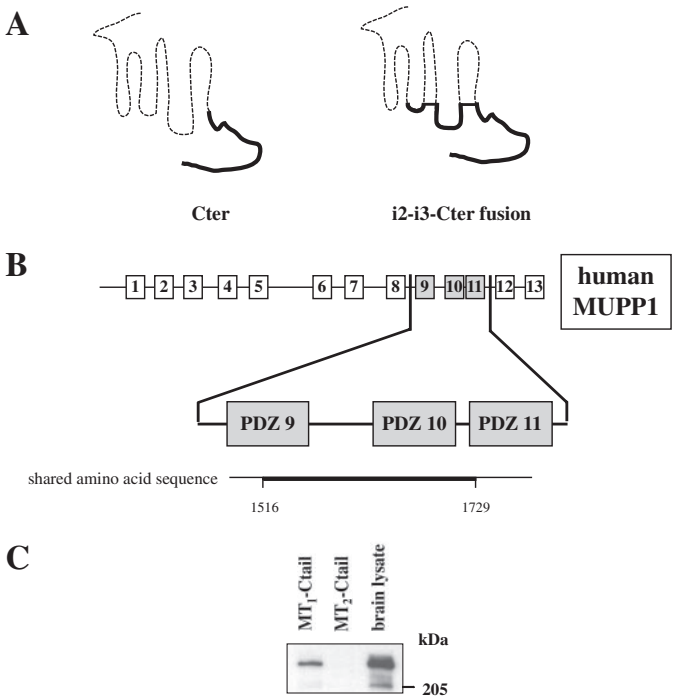

FIGURE 1. **The C-tail of MT_1 interacts with MUPP1.** *A*, schematic representation of melatonin receptor baits (C-tail or a fusion of the i2 loop, i3 loop, and C-tail) used in the yeast two-hybrid screen. *B*, screening of a human brown adipocyte cDNA library with MT_1 baits identified 14 different sequences corresponding to the indicated region of MUPP1. The sequence shared by all clones is indicated in boldface type (nucleotides 4548–5189, amino acids 1516–1729). *C*, solubilized brain proteins were incubated with the immobilized His_6-tagged C-tail of MT_1 or MT_2. The presence of MUPP1 among the retained proteins was evaluated by Western blotting with anti-MUPP1 antibodies.

brown adipocytes, a cellular context known to express functional melatonin receptors (31). Among the positive clones that interacted with the two baits containing the C-tail of MT_1, we identified 14 sequences corresponding to the multi-PDZ protein MUPP1 (Fig. 1*B*), which is composed of 13 PDZ domains (32). Sequence alignment of these clones unraveled a common region corresponding to nucleotides 4548–5189 (amino acids 1516–1729) in the coding sequence of the human MUPP1 encompassing part of PDZ9 and PDZ11 and the entire PDZ10 domain. The identification of a PDZ domain-containing protein as a specific interacting partner of the C-tail of MT_1 is consistent with the presence of a canonical class III PDZ domain-binding motif DSV-COO^- at the COOH terminus. To further test the specificity of our yeast two-hybrid screen, we used the C-tail of the β_2-adrenergic receptor as bait. Despite the presence of a functional PDZ binding motif at the C-tail of this receptor, we were unable to recover MUPP1, indicating the high specificity of the MT_1/MUPP1 interaction (data not shown).

To confirm the interaction between the C-tail of MT_1 and MUPP1 in a different experimental setting, we incubated MT_1 or MT_2 C-tails, which were chemically synthesized with a His_6 tag and immobilized on beads, with whole brain lysates from mice. We then tested for the presence of MUPP1 among the retained proteins with anti-MUPP1 antibodies (Fig. 1*C*). MUPP1 was bound to the C-tail of MT_1 but not to that of MT_2, confirming the specificity of the interaction.

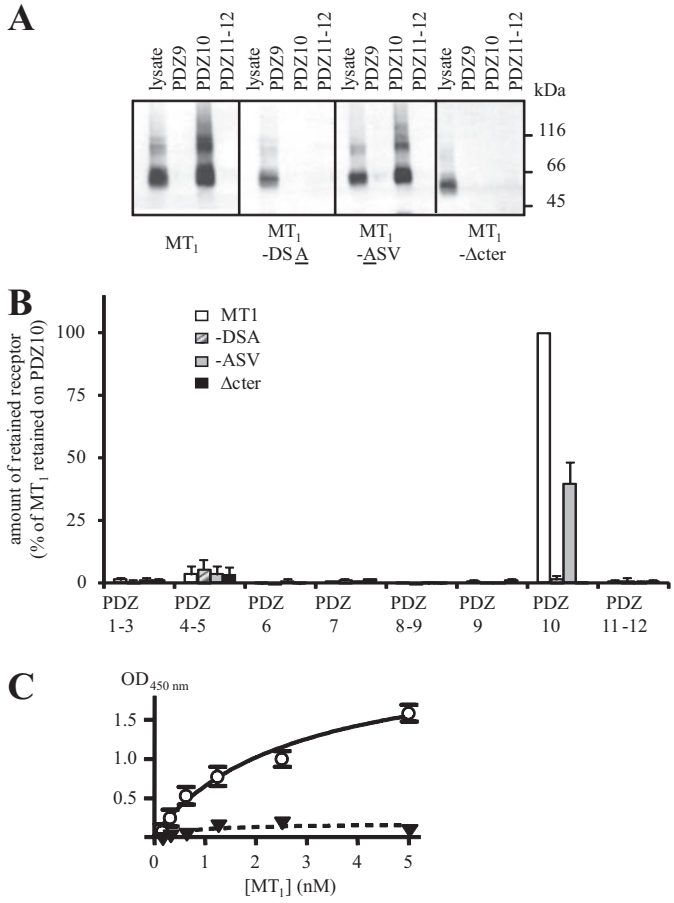

FIGURE 2. **Affinity and molecular determinants of the MT_1/MUPP1 interaction.** *A*, *in vitro* GST pull-down assay using lysates of HEK293 cells expressing the indicated receptors with GST-PDZ9, PDZ10, or PDZ11-12. Affinity constants (K_D) of the receptors for [^{125}I]MLT are 136 ± 8 pM (MT_1), 321 ± 50 pM (MT_1-DSA), 220 ± 38 pM (MT_1-ASV), and no specific binding (MT_1-Δcter). *B*, ELISA using adsorbed GST-fused PDZ domains of MUPP1 for interaction with solubilized MT_1, MT_1-DSA, MT_1-ASV, or MT_1-Δcter. *C*, ELISA saturation assay to determine the affinity of PDZ10 for MT_1. Increasing amounts of solubilized FLAG-MT_1 (quantified by [^{125}I]MLT binding) were incubated on adsorbed GST-PDZ10 (○) or GST-PDZ9 (▲). Data are means ± S.E. of at least three independent experiments each performed in duplicate (*B* and *C*) or are representative of two further experiments (*A*).

Affinity and Molecular Determinants of the MT_1/MUPP1 Interaction—To delineate the molecular determinants of the MT_1/MUPP1 interaction *in vitro*, we used receptor mutants of the PDZ binding motif and GST fusion proteins of the different PDZ domains of MUPP1 (Fig. 2*A*) to perform GST pull-down experiments (see supplemental Fig. S1 for GST constructs). Only GST-PDZ10 was able to specifically precipitate the NH_2-terminally FLAG-tagged MT_1, confirming that this domain is involved in the interaction. Mutation of the very last valine residue into alanine (MT_1-DSA) completely abolished the interaction, as did the deletion of the entire C-tail (MT_1-Δcter). Mutation of the aspartate residue at position −2 (MT_1-ASV) reduced the amount of precipitated receptor.

To confirm these interactions in a more quantitative assay, we used an ELISA set-up where similar quantities of the GST-PDZ fusion proteins were immobilized (Fig. 2*B*) and incubated with equivalent quantities of solubilized receptors, as confirmed by Western blot (not shown). Only PDZ10 was able to interact with MT_1. Although the MT_1-ASV mutant was partially retained, MT_1-Δcter and MT_1-DSA completely failed to interact with PDZ10. We then determined the dissociation constant (K_d) of the MT_1/PDZ10 interaction with the ELISA (Fig. 2*C*). Whereas binding to immobilized PDZ10 was saturable and of high affinity (K_d = 3.8 ± 0.7 nM), only background binding was detected for PDZ9-coated wells.

Overall, our *in vitro* data show that MUPP1 interacts with MT_1 with high affinity and that this interaction involves the PDZ10 domain of MUPP1 and the COOH-terminal DSV motif of MT_1. The interaction mainly depends on the COOH-terminal valine residue, although other amino acids, such as the aspartate residue at position −2, also appear to be involved.

Interaction between MT_1 and MUPP1 in Mammalian Cells—To investigate the interaction of MUPP1 with MT_1 in mammalian cells, we expressed HA-tagged MUPP1 in HEK-FLAG-MT_1 cells (100 fmol/mg of protein) (25). As shown by immunofluorescence staining with anti-HA antibodies, a small amount of MUPP1 was present throughout the cytoplasm, but the majority was located at the plasma membrane, where it colocalized with MT_1 (Fig. 3, *A–C*). The interaction of both proteins was addressed in intact cells by co-immunoprecipitation experiments in HEK-FLAG-MT_1 cells. As shown in Fig. 3*D*, anti-FLAG antibodies coprecipitated endogenous MUPP1.

To demonstrate the presence of the protein complex in native tissue, we performed immunoprecipitation studies with ovine pituitary PT tissue samples known to express significant amounts of endogenous MT_1 receptors (33) and MUPP1 (data not shown). Receptors were labeled with the specific [^{125}I]MLT radioligand, and protein complexes were solubilized and immunoprecipitated with anti-MUPP1 antibodies. As shown in Fig. 3*E*, significant amounts of radiolabeled MT_1 were precipitated in the presence of anti-MUPP1 as compared with irrelevant control antibodies, demonstrating the existence of MT_1-MUPP1 complexes in native tissue.

To further confirm the specificity of the interaction, we transiently expressed similar levels of FLAG-MT_1, FLAG-MT_1-ASV, FLAG-MT_1-DSA, or FLAG-MT_1-Δcter with HA-MUPP1 (Fig. 3*F*). In agreement with our *in vitro* interaction data, HA-MUPP1 was readily precipitated from cells expressing FLAG-MT_1, to a lesser extent from cells expressing FLAG-MT_1-ASV, and not at all from cells expressing FLAG-MT_1-DSA, FLAG-MT_1-Δcter, or HA-MUPP1 alone (Fig. 3*G*). The amount of co-precipitated MUPP1 did not change upon stimulation (up to 10 min) with 10 nM melatonin (MLT), the natural hormone of MT_1 (Fig. 3*H*). Taken together, these results show that MUPP1 and MT_1 interact constitutively in HEK 293 cells and in the PT.

Effect of PDZ10 on MT_1 Internalization and Degradation—Interaction of GPCRs with PDZ proteins has been shown to stabilize receptors by inhibiting either their constitutive or agonist-promoted internalization (8, 34) or by interfering with receptor degradation (4, 5). To study the role of MUPP1 in MT_1 internalization and degradation, we used the isolated PDZ10 domain of MUPP1 as a dominant negative to disrupt the MUPP1/MT_1 interaction. As shown in Fig. 4*A*, the amount of MUPP1 associated with the receptor is, as expected, strongly decreased in the presence of PDZ10. We first determined the rate of constitutive internalization of MT_1 in the absence and

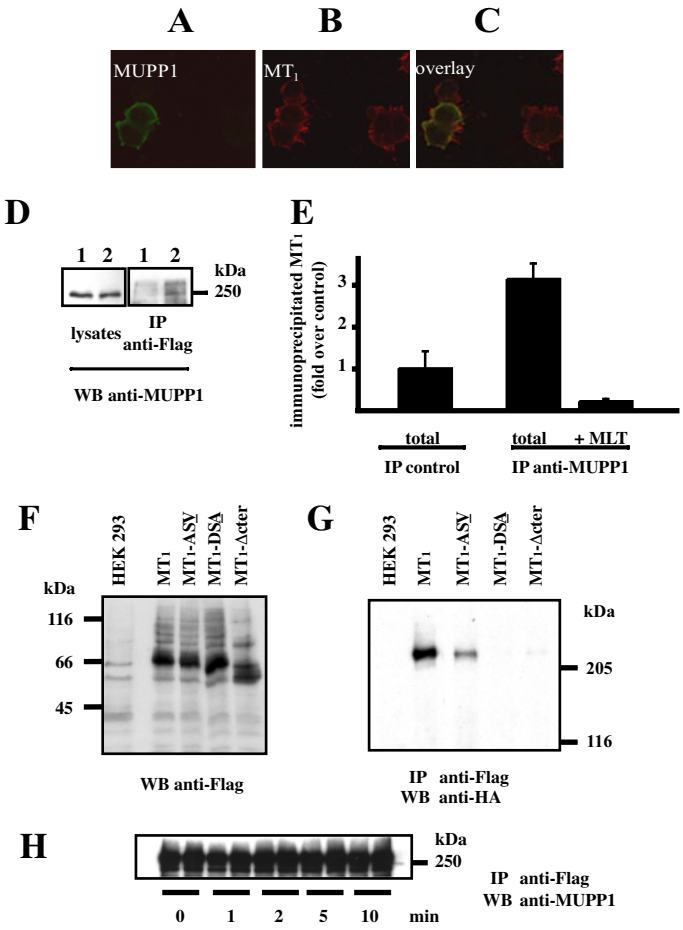

FIGURE 3. **Interaction between MUPP1 and MT_1 in mammalian cells.** *A–C*, confocal images of HEK293 cells showing a partial localization of HA-MUPP1 and FLAG-MT_1 at the plasma membrane. FLAG-MT_1 and HA-MUPP1 were detected by immunofluorescence using anti-FLAG or anti-HA antibodies. *D*, co-immunoprecipitation (*IP*) of endogenous MUPP1 in HEK-FLAG-MT_1 (*lane 2*) or HEK 293 cells (*lane 1*). Data are representative of at least two further experiments. *E*, co-immunoprecipitation of MT_1 with MUPP1 in ovine pituitary pars tuberalis; [^{125}I]MLT-labeled receptors (~45 fmol/mg membrane proteins) were immunoprecipitated from solubilized membranes by anti-MUPP1 antibodies or control rabbit sera (pool of five preimmune rabbit sera). Nonspecific immunoprecipitated binding was evaluated in the presence of 1 μM MLT. *F* and *G*, lysates from HEK 293 cells expressing HA-MUPP1 alone or with FLAG-MT_1, FLAG-MT_1-ASV, FLAG-MT_1-DSA, or FLAG-MT_1-Δcter were prepared (*F*), receptors were immunoprecipitated, and precipitates were analyzed by Western blot (*WB*) for the presence of MUPP1 (*G*). *H*, time course of MLT (10 nM) stimulation in HEK-FLAG-MT_1 cells transfected with HA-MUPP1. Western blot analysis of HA-MUPP1 was performed on anti-FLAG immunoprecipitates by anti-HA antibodies (*G*) or anti-MUPP1 antibodies (*F*). Data are representative of at least two further experiments.

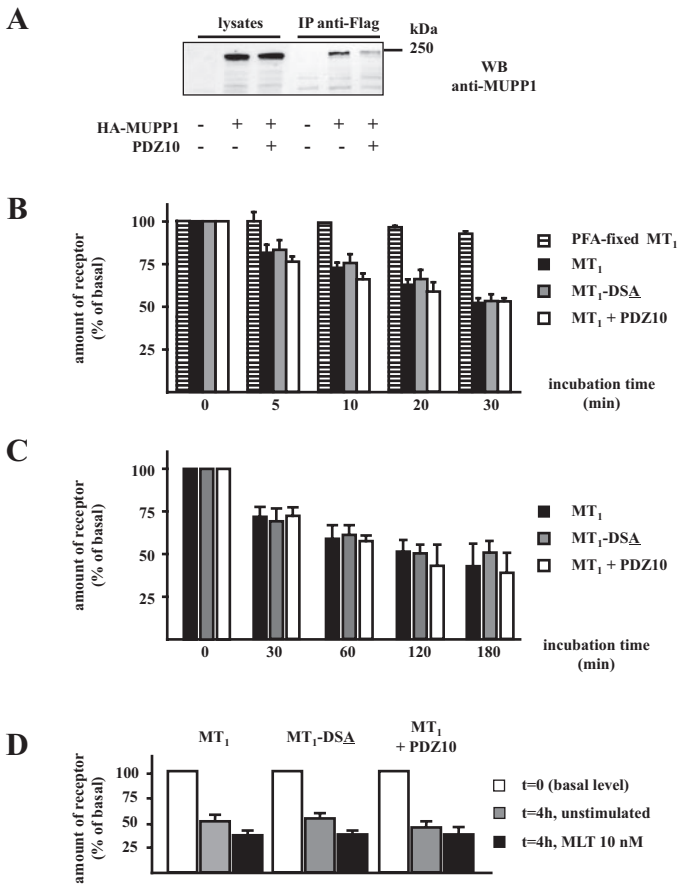

FIGURE 4. **Effect of PDZ10 on MT_1 internalization and degradation.** *A*, competition of PDZ10 with MUPP1 for binding to FLAG-MT_1. Lysates from HEK-FLAG-MT_1 cells expressing the indicated proteins were prepared, and FLAG-MT_1 was immunoprecipitated (*IP*). Lysates and immunoprecipitates were separated by SDS-PAGE, and analysis was performed by Western blot (*WB*) using anti-HA antibodies. *B*, constitutive internalization of MT_1; HEK-FLAG-MT_1 cells (*black bars*) or expressing PDZ10 (*white bars*) and HEK-MT_1-DSA cells (*gray bars*) were preincubated on ice with monoclonal anti-FLAG antibody and then transferred to 37 °C for the indicated times. Remaining cell surface receptors were quantified by fluorescence-activated cell sorting. To exclude the possibility that the observed decrease in fluorescence is due to an artifactual dissociation of the anti-FLAG antibody, receptor internalization was inhibited by fixation with 4% paraformaldehyde before incubation with anti-FLAG antibody (*hatched bars*). The constant signal validates our assay. *C*, agonist-stimulated internalization of MT_1; HEK-FLAG-MT_1 cells (*black bars*) or expressing PDZ10 (*white bars*) and HEK-MT_1-DSA cells (*gray bars*) were stimulated with MLT (10 nM) for the indicated times and fixed, and the remaining cell surface receptors were quantified by fluorescence-activated cell sorting. *D*, MT_1 degradation; HEK-FLAG-MT_1 cells (*black bars*) or expressing PDZ10 (*white bars*) and HEK-MT_1-DSA cells (*gray bars*) were pretreated with cycloheximide (100 μM) for 45 min. The treatment was continued in the absence or presence of MLT (10 nM) for 4 h. The total amount of FLAG-MT_1 was quantified by immunodetection. Data are means ± S.E. of three independent experiments, each performed in duplicate (*B–D*), or are representative of two further experiments (*A*).

presence of PDZ10. Fig. 4*B* shows that the rate of internalization is not affected in the presence of PDZ10; in addition, the MT_1-DSA mutant, unable to interact with MUPP1, presents equivalent constitutive internalization characteristics. Similarly, the binding of MUPP1 to MT_1 appears not to alter ligand-induced receptor internalization by 100 nM MLT, since equivalent internalization kinetics and maximal internalization of ~60% within 3 h were observed in the absence and presence of PDZ10 (Fig. 4*C*) and for the MT_1-DSA mutant. The degradation of MT_1 was studied by treating cells with the protein synthesis inhibitor cycloheximide (100 μM) for 4 h. The more than 50% decrease in receptor number, in the absence of MLT, suggests that constitutively internalized receptors are mostly degraded. Simultaneous MLT treatment (100 nM) moderately increased MT_1 degradation (Fig. 4*D*). Similar effects were observed for MT_1-DSA. Coexpression of PDZ10 did not modify unstimulated and MLT-stimulated MT_1 degradation. These results indicate that MUPP1 has no significant effect on MT_1 endocytosis and degradation.

MUPP1 Is Necessary for Signaling of MT_1 through the Adenylyl Cyclase Pathway—MT_1 is a predominantly G_i-coupled GPCR that inhibits adenylyl cyclase (AC) activity in primary cell cultures and transfected cells (29, 35). Stimulation of HEK-

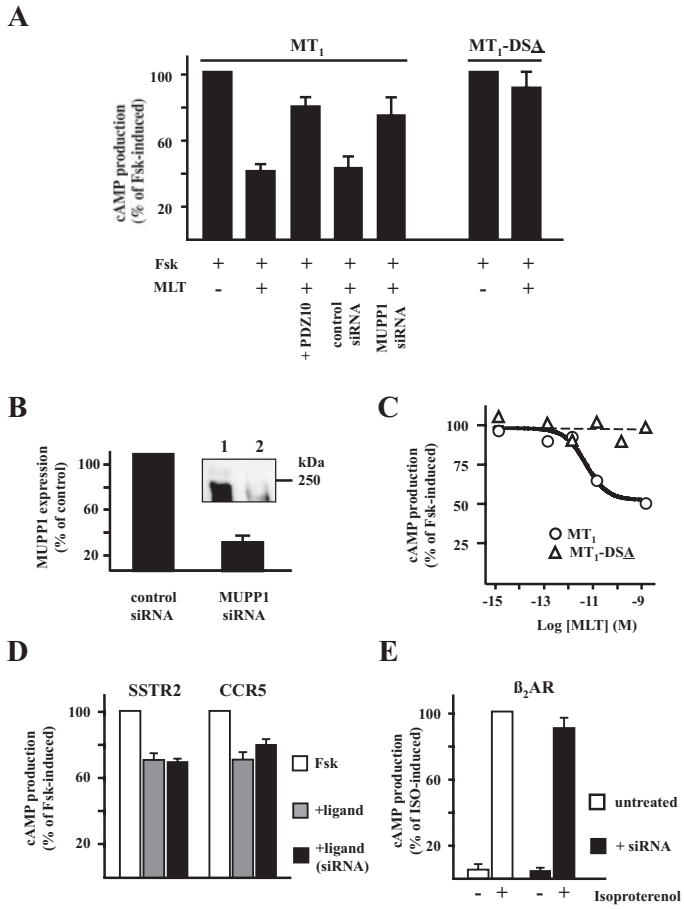

FIGURE 5. **Signaling of MT_1 through adenylyl cyclase depends on the presence of MUPP1.** *A*, HEK-FLAG-MT_1 cells transfected with the indicated cDNAs or siRNA duplexes or FLAG-MT_1-DSA cells were stimulated with MLT (10 nM) or not in the presence of 1 μM forskolin (*Fsk*), and intracellular cAMP levels were determined. *B*, inhibition of endogenous MUPP1 expression. HEK-FLAG-MT_1 were transfected with a scrambled control siRNA (*lane 1*) or MUPP1-specific siRNA duplexes (*lane 2*). Lysates were immunoprecipitated with anti-FLAG antibody, and MUPP1 was revealed by anti-MUPP1 antibodies. *C*, dose-response curves of MLT-induced inhibition of forskolin-stimulated cAMP production in HEK-FLAG-MT_1 and FLAG-MT_1-DSA cells (curves from a single experiment representative of at least three other independent experiments). EC_{50} = 16.6 ± 9.8 pM for HEK-FLAG-MT_1. *D*, cAMP response induced by the ligand in Fsk-stimulated HEK293 cells (1 μM) transiently transfected with the G_i-coupled somatostatin receptor SSTR2 or chemokine receptor CCR5 (10 nM somatostatin or 100 nM RANTES, respectively) or the G_s-coupled β_2-adrenergic receptor (β_2AR) (1 μM isoproterenol) in the absence or presence of MUPP1 siRNA. Data are means ± S.E. of at least three independent experiments, each performed in triplicate.

FLAG-MT_1 cells with a saturating MLT concentration (10 nM) resulted in the expected decrease of forskolin-stimulated cAMP levels of about 60% (Fig. 5*A*). Expression of the dominant negative PDZ10 in these cells strongly attenuated the inhibitory effect of MT_1 on cAMP production, indicating that binding of MUPP1 to MT_1 is necessary for efficient coupling of the receptor to the cAMP pathway. To verify that the displaced protein corresponds to MUPP1, we treated cells with MUPP1-specific siRNA molecules. MUPP1 expression was decreased by nearly 80% compared with the control siRNA (Fig. 5*B*), and the MLT-induced decrease in cAMP production was abolished to the same extent as in cells expressing the dominant negative PDZ10 domain (Fig. 5*A*). Importantly, control siRNA molecules did not interfere with the inhibitory effect of MLT on forskolin-stimulated cAMP levels. This strongly suggests that binding of MUPP1 to the MT_1 C-tail is essential for its efficient coupling to the AC pathway. To further support this idea, we tested the MT_1-DSA mutant, which is unable to interact with MUPP1. Consistently, 10 nM MLT stimulation of HEK 293 cells stably expressing MT_1-DSA receptors at similar expression levels as HEK-FLAG-MT_1 cells did not inhibit forskolin-stimulated cAMP levels (Fig. 5, *A* and *C*). To further assess the specificity of the MUPP1 interaction with MT_1 on the AC pathway, we measured the effect of MUPP1 knockdown on two other G_i-coupled receptor, the human SSTR2 somatostatin receptor and the CCR5 chemokine receptor. Indeed, MUPP1 siRNA treatment of cells transiently transfected with each of these receptors had no effect on the cAMP inhibition elicited by 10 nM somatostatin or 100 nM RANTES, respectively (Fig. 5*D*). In addition, the siRNA treatment had no effect on the cAMP response observed for the β_2-adrenergic receptor, a G_s-coupled receptor, stimulated by 1 μM isoproterenol (Fig. 5*D*). Overall, our results show that binding of MUPP1 to the COOH-terminal DSV motif of MT_1 plays a central role in MT_1 signaling through the AC pathway.

G_i Coupling and High Affinity Agonist Binding to MT_1 Depends on the Presence of MUPP1—We hypothesized that the inability of FLAG-MT_1 to couple to the AC pathway in the absence of MUPP1 may be due to a defect in G_i coupling to the receptor. In agreement with previous reports (29), solubilization of MT_1 under mild conditions preserved the interaction with $G\alpha_i$ proteins (Fig. 6*A*). In contrast, coexpression of PDZ10 strongly decreased the quantity of coprecipitated G_i. Consistently, in cells stably expressing the MUPP1 binding-deficient FLAG-MT_1-DSA mutant, $G\alpha_i$ proteins were undetectable under these conditions. Decreased G protein coupling was specific for $G\alpha_i$, since $G\alpha_q$ was readily precipitated under all conditions. These results show that the inability of MT_1 to signal through the AC pathway in the absence of MUPP1 is most likely due to its reduced G_i coupling capacity.

Previous studies have shown that high affinity agonist binding to MT_1 depends on the coupling of the receptor to G_i proteins (36). Accordingly, decreased high affinity agonist binding would be expected when MUPP1 is displaced from MT_1. We therefore incubated cell membranes prepared from HEK-FLAG-MT_1 cells in the presence or the absence of purified PDZ9 or PDZ10 and determined agonist binding using the radiolabeled MLT receptor agonist [^{125}I]MLT (Fig. 6*B*). In the absence of added PDZ domain, MT_1 bound [^{125}I]MLT with the expected high affinity (K_D = 136 ± 8 pM). Similar results were obtained in the presence of PDZ9 (K_D = 160 ± 15 pM). In contrast, in the presence of PDZ10, a significantly lower affinity was observed (K_D = 378 ± 79 pM) ($p < 0.05$; MT_1 alone *versus* MT_1 + PDZ10). The number of binding sites was not affected in any of the conditions (B_{max} = 100 ± 9, 94 ± 9, and 118 ± 13% for MT_1, MT_1 + PDZ9, and MT_1 + PDZ10, respectively). The lower affinity for [^{125}I]MLT in the presence of PDZ10 is consistent with the lower affinity of the MT_1-DSA mutant (K_D = 321 ± 50 pM), which is devoid of MUPP1 binding. These results indicate that binding of MUPP1 to the MT_1 C-tail participates in high affinity agonist binding, most likely by stabilizing G_i binding to the agonist-activated receptor.

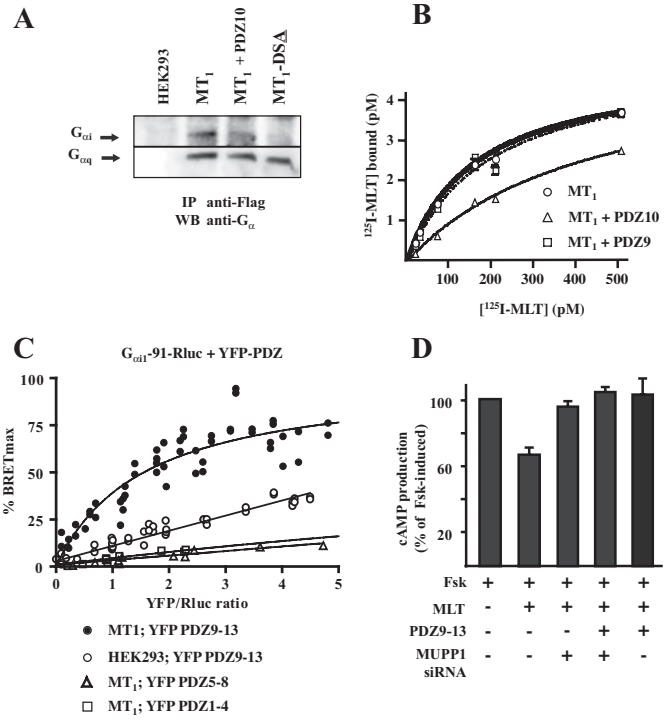

FIGURE 6. **Effect of MUPP1 on G protein coupling to MT_1.** *A*, nontransfected HEK 293 cells or HEK-FLAG-MT_1 cells expressing or not expressing PDZ10 or HEK 293 cells expressing FLAG-MT_1-DSA were stimulated with MLT (10 nM) for 30 min and solubilized. Lysates were immunoprecipitated (*IP*), and precipitates were analyzed by Western blot (*WB*) with Gα-specific antibodies. Data are representative of two further experiments. *B*, [^{125}I]MLT saturation binding experiment on membranes prepared from HEK-FLAG-MT_1 cells performed in the absence (○ + *boldface line*) or the presence of 2 μg/ml PDZ9 (□) or PDZ10 (△). Data are means ± S.E. of at least three independent experiments, each performed in duplicate. *C*, BRET donor saturation curves were generated in HEK-FLAG-MT_1 cells (●, △, and □) or HEK 293 cells (○) by transfecting a constant DNA amount of $G\alpha_{i1}$-91-Rluc and increasing quantities of the YFP-tagged PDZ fusion proteins. The BRET, total luminescence, and total fluorescence were measured. The curve obtained for the BRET acceptor YFP-PDZ9–13 in HEK-FLAG-MT_1 cells (●), was best fitted with a nonlinear regression equation assuming a single binding site. Curves obtained for YFP-PDZ1–4 (□) and YFP-PDZ5–8 (△) in HEK-FLAG-MT_1 and YFP-PDZ9–13 in HEK 293 cells (○) were best fitted with a linear regression equation. The curves represent 3–5 individual saturation experiments. *D*, MLT-promoted (10 nM) cAMP response was measured in HEK293 cells stimulated with 1 μM Fsk transiently transfected with FLAG-MT_1 alone or co-transfected with PDZ9–13 and treated or not with MUPP1 siRNA. Data are means ± S.E. of at least three independent experiments, each performed in triplicate.

To show the formation of a trimeric complex between MT_1, G_i, and MUPP1, we used the BRET assay, which allows detection of real time protein interactions in a cellular context (54). The previously described $G\alpha_{i1}$-91-Rluc fusion protein (energy donor) (37) was coexpressed with a fragment of MUPP1 comprising PDZ domains 9–13 fused at its amino-terminal tail to the energy acceptor YFP (YFP-PDZ9–13).

Expression of both proteins in HEK 293 cells revealed a nonspecific interaction between G_i and MUPP1 (weak signal, linear and nonsaturating behavior of BRET donor saturation curve) (Fig. 6*C*). In contrast, when YFP-PDZ9–13 and $G\alpha_{i1}$-91-Rluc were expressed in HEK-FLAG-MT_1 cells, G_i interacted with high affinity with MUPP1 as shown by the hyperbolic and saturable behavior of the BRET donor saturation curve. Stimulation of cells with MLT did not alter BRET signals (not shown). The high affinity interaction between G_i and YFP-PDZ9–13 was specific, since no interaction was observed for YFP-PDZ1–4 and YFP-PDZ5–8 constructs in HEK-FLAG-MT_1 cells. To evaluate the functional importance of the PDZ9–13 subdomain on the AC pathway, we co-transfected FLAG-tagged MT_1 and PDZ9–13 in HEK293 cells devoid of MUPP1 (MUPP1 siRNA-treated). Although the MLT-promoted inhibition of Fsk-stimulated cAMP production was abolished in MUPP1 siRNA-treated cells as expected, simultaneous expression of PDZ9–13 did not allow us to reestablish the MT_1 response (Fig. 6*D*). Indeed, PDZ9–13 by itself inhibits the MT_1 response, as was observed for the single PDZ10 fragment. Collectively, our results indicate that the PDZ9–13 fragment of MUPP1 is necessary for high affinity binding of $G\alpha_i$ to MT_1 but not sufficient to reconstitute a functional system to modulate the AC pathway.

Disruption of MUPP1/MT_1 Interaction Affects MLT-stimulated ERK Activation—Many GPCRs activate the mitogen-activated protein kinase pathway, although through several different mechanisms (38). A common mechanism of mitogen-activated protein kinase activation involves $G_\beta\gamma$ subunits that are released from G_i proteins upon receptor activation. To determine whether the mitogen-activated protein kinase activation by MT_1 also involves G_i proteins, we treated HEK-FLAG-MT_1 cells with pertussis toxin (PTX; 10 ng/ml), which is known to inactivate G_i proteins. As shown in Fig. 7*A*, 10 nM MLT-promoted ERK phosphorylation was abolished in PTX-treated cells, indicating that ERK activation by MT_1 is indeed G_i-dependent. We studied the kinetics of ERK phosphorylation in the presence and absence of PDZ10, to determine the effect of MUPP1 on ERK activation. In both cases, the amplitude and time course of ERK activation was similar with maximal effects at 5 min of MLT stimulation (Fig. 7, *B* and *C*). Similar B_{max} and EC_{50} values were obtained for the MT_1 wild-type and the MUPP1 binding-deficient MT_1-DSA mutant (Fig. 7, *C* and *D*). These results suggest that G_i-dependent ERK signaling of MT_1 is not altered in the absence of MUPP1 binding. Such an observation is in apparent contradiction to our data on the cAMP pathway. To account for the different effect of MUPP1 on both pathways, we then hypothesized that the AC pathway can be more sensitive to alterations of the G_i coupling to MT_1 than the mitogen-activated protein kinase pathway. We therefore decreased the amount of functional G_i proteins by incubating cells with increasing doses of PTX and determined the degree of MLT-promoted ERK phosphorylation of wild-type MT_1 or the MT_1-DSA mutant (Fig. 7*E*). Maximal doses of PTX inhibited ERK activation for both receptors to a similar extent. This shows that the ERK activation of the MT_1-DSA mutant also depends on G_i protein activation and excludes the possibility that ERK activation becomes G_q-dependent in the absence of functional G_i coupling. At submaximal PTX concentrations, ERK activation by the MT_1-DSA mutant and the wild-type receptor was clearly different (IC_{50} = 0.10 and 0.02 ng/ml for wild-type MT_1 and MT_1-DSA, respectively). The left shift of the dose-response curve of ERK phosphorylation of the MT_1-DSA mutant indicates that ERK activation becomes indeed more sensitive to the amount of active G_i proteins in the absence of MUPP1 binding to MT_1. Taken together, both G_i-dependent signaling pathways, the AC and the ERK pathways, are affected in the absence of MUPP1 binding to MT_1.

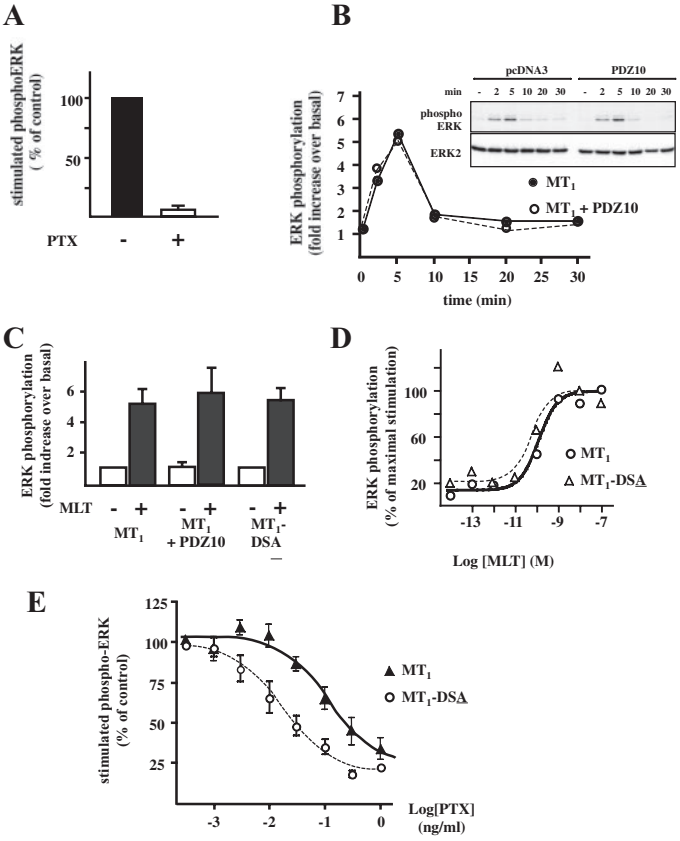

FIGURE 7. **Disruption of the MUPP1/MT_1 interaction affects agonist-stimulated ERK activation.** *A*, HEK-FLAG-MT_1 cells were pretreated overnight with PTX (10 ng/ml) and stimulated with MLT (10 nM) for 5 min, and ERK activation was determined by Western blotting using phospho-ERK-specific antibodies. *B*, kinetics of MLT-promoted ERK activation (10 nM MLT) in HEK-FLAG-MT_1 cells expressing PDZ10 (○) or not (●). ERK activation was normalized to ERK2 expression. *C*, comparison of maximal MLT-promoted ERK phosphorylation (*black bars*) and basal levels (*white bars*) in cells expressing MT_1 with or without PDZ10 and MT_1-DSA. *D*, dose response of MLT-induced ERK-phosphorylation at 5 min in FLAG-MT_1-expressing (○) or MT_1-DSA-expressing (△) cells (graph of a single representative experiment of three; EC_{50} = 0.27 ± 0.18 nM for MT_1 and 0.26 ± 0.19 nM for MT_1-DSA). *E*, dose response of PTX overnight pretreatment (0.3 pg/ml to 1 ng/ml) on MLT-promoted ERK phosphorylation (10 nM, 5 min) in FLAG-MT_1-expressing (▲) or MT_1-DSA-expressing (○) cells.

DISCUSSION

We show here that the PDZ protein MUPP1 regulates GPCR signaling by stabilizing the coupling of G proteins to their cognate receptors. This substantially extends the role of MUPP1 in GPCR function, which was previously limited to the subcellular targeting and trafficking of receptors. The PDZ10 domain of MUPP1 is the only one out of its 13 PDZ domains that specifically associates with the C-tail of the MT_1 but not with that of the MT_2 and the β_2-adrenergic receptor. The valine of the canonical class III PDZ domain binding motif DSV of the C-tail of MT_1 is crucial for the high affinity interaction. Using several approaches to hamper the MUPP1/MT_1 association (overexpression of PDZ10 as a MUPP1 competitor, extinction of MUPP1 expression by siRNA, or expression of the MUPP1 binding-deficient MT_1-DSA mutant), we were able to destabilize the interaction of G_i proteins with MT_1 and to interfere with G_i-dependent signaling pathways. Indeed, MLT-stimulated AC inhibition and ERK activation were differentially affected when the binding of MUPP1 to MT_1 was impaired.

PDZ scaffolds have been shown to modulate GPCR signaling in different ways. Binding of GPCRs to PDZ scaffolds has been reported to modulate the amount of receptor at the cell surface and consequently the amplitude of the functional response by altering the receptor's trafficking and stability (2). Other examples highlight the importance of the scaffolding properties of PDZ domain proteins in GPCR signaling. For instance, simultaneous binding of the PDZ scaffold GIPC to the G_i-coupled D_2 dopamine receptor and to RGS19 favors the GDP/GTP exchange of G_i by RGS19 (17). Moreover, binding of NHERF-1 to GPCRs and phospholipase Cβ3 enhances the signaling efficiency of the phospholipase Cβ/Ca^{2+} pathway (13–15). Modulation of MT_1 signaling by MUPP1 probably involves a previously unappreciated regulatory mechanism. Disruption of the interaction of MUPP1 with the C-tail of MT_1 decreased signaling of MT_1 through the AC and the ERK pathway. Importantly, the interaction between G_i proteins and MT_1 was also destabilized under these conditions, suggesting that MUPP1 regulates MT_1 signal transduction by stabilizing the receptor-G_i protein complex. This indicates physical proximity between MUPP1 and G_i proteins, as supported by our BRET experiments. However, more complex mechanisms cannot be excluded, since PDZ9–13, which is able to restore high affinity binding of G_i to MT_1, is insufficient to reconstitute functional coupling to AC. Some PDZ proteins are indeed able to physically interact with heterotrimeric G proteins, as recently reported for PSD95, SAP97, and Veli2, which interact with Gγ_{13} (39). Furthermore, α-syntrophin has been shown to bind to $G_\beta\gamma$ through its PDZ domain (40). Although Gβ subunits typically code for the "LWL" or "IWN" sequence at their C-tails, several Gγ subunits (*e.g.* Gγ_4, Gγ_{12}, and Gγ_{13}) have the COOH-terminal "TIL" sequence, which corresponds to the class I ((S/T)*X*L) PDZ domain recognition sequence. Alternatively, MUPP1 and G_i may be physically linked through a third protein. According to our BRET experiments, the domain that promotes G_i binding to MT_1 appears to localize between PDZ9 and PDZ13, since this part of MUPP1 is sufficient to stabilize the ternary complex between MUPP1, G_i, and MT_1.

The association of MUPP1 with MT_1 may participate in the high stability of the MT_1-G_i protein complex. G_i has been shown to be precoupled to MT_1 in its inactive form and to remain stably associated upon agonist stimulation despite the presence of high GTP concentrations in intact cells (29, 36). Destabilization of the MT_1-G_i complex in the absence of MUPP1 has different effects on the signaling capacities of MT_1. Whereas MUPP1 is necessary for efficient coupling of MT_1 to the AC pathway, the PTX-sensitive ERK activation is only moderately affected (only when the amount of G_i proteins becomes limiting). This highlights the potential regulatory role of MUPP1 in the modulation of MT_1 signaling.

MT_1 is not the only GPCR that binds to MUPP1. The serotonin 5-HT_{2C} receptor was the first GPCR that has been shown to interact with MUPP1 (41). Although possibly regulated by the phosphorylation state of the receptor, the functional role of 5-HT_{2C} binding to PDZ10 of MUPP1 still remains poorly defined (42). Whereas MT_1 and 5-HT_{2C} bind to the same PDZ domain (PDZ10), their G protein coupling profiles are different. MT_1 couples preferentially to G_i, and 5-HT_{2C} couples pref-

TABLE 1
Proteins found to interact with the PDZ10 domain of MUPP1

PDZ class[a]	Interacting protein	COOH-terminal sequence	Reference/source
I	Ad9 4-ORF1	-KIATLV	Ref. 23
I	TAPP1	-LPVSDV	Ref. 55
I	TAPP2	-IRTSDV	Ref. 55
I	5HT2a	-EKVSCV	Ref. 41
I	5HT2b	-EQVSYV	Ref. 41
I	5HT2c	-ERISSV	Ref. 41
III	Claudin-1	-SGKDYV	Ref. 56
III	Claudin-3	-DRKDYV	Ref. 43
III	Claudin-14	-RLNDYV	Ref. 43
Other	KNCE 4.1	-GLVSIC	Ref. 43
I	NAV1.4	-VKESLV	Ref. 43
I	PKC-α	-ILQSAV	Ref. 43
I	Sema4b	-IRDSVV	Ref. 43
II	SSTR2b	-DIIAWV	Ref. 43
III	c-Kit	-LVHDDV	Ref. 24
III	MT_1	-VKVDSV	Ref. 43 and present report

[a] Class I, (S/T)*Xψ*; class II, *ψXψ*; class III, (D/E/K/R)*Xψ*; other, *XXC* or X*ψ*(D/E), where *ψ* represents a hydrophobic residue (53).

erentially to G_q. This difference may explain why the disruption of MUPP1 binding to 5-HT_{2C} does not abolish receptor signaling as for MT_1. This interpretation is consistent with our observation that only coupling to G_i and not G_q is affected in the absence of MUPP1 binding to MT_1.

The metabotropic γ-aminobutyric acid B ($GABA_B$) receptor 2 has also been reported to interact with MUPP1 (5). In contrast to MT_1 and 5-HT_{2C}, metabotropic $GABA_B$ receptor 2 binds to the PDZ13 domain of MUPP1. Accordingly, binding to this PDZ domain has different consequences for receptor function, namely the stabilization of the metabotropic $GABA_B$ receptor 2 and the enhancement of the duration of receptor signaling. Although other PDZ proteins have also been shown to stabilize their respective binding partners, the underlying mechanism remains unknown. The C-tails of further GPCRs have been reported to bind to MUPP1 in *in vitro* assays, such as 5-HT_{2A}, 5-HT_{2B} (41), and the mouse SSTR2b somatostatin receptor splice variant (43). The *in vivo* relevance and the functional consequences of these interactions remain to be determined.

The constitutive nature of the MT_1/MUPP1 interaction raises the question of its regulation. The PDZ10 domain of MUPP1 is the target of multiple proteins (see Table 1). This implies that the selection of PDZ10 binding partners is highly competitive and will depend on their relative affinities and expression levels. Similarly, other PDZ proteins can bind to MT_1[6] and are consequently expected to compete with MUPP1 for MT_1 binding. This may be functionally relevant, since different PDZ proteins can differentially modulate receptor function (44). Furthermore, the MT_1/MUPP1 interaction may be regulated by the expression level of MUPP1 itself. Despite the widespread expression of MUPP1 in the brain (45) and at multiple peripheral sites, its expression may vary depending on the cellular context and different pathological conditions. For instance, human keratinocyte infection by papillomavirus HPV18 E6 has been shown to induce epithelial hyperplasia and massive down-regulation of MUPP1 by targeting MUPP1 to the proteasome (23, 46, 47). During adenovirus infection by Ad9E4, responsible for estrogen-dependent mammary tumors in rat, the viral protein ORF1 has been shown to promote cytoplasmic sequestration of MUPP1 (23, 48). In both cases, MUPP1 is removed far from its potential membrane partners, thus impeding any interaction with them. Regulation of the MT_1/MUPP1 interaction is likely to occur under these circumstances, since functional MT_1 expression has been shown in keratinocytes (49) and mammary tumors (50). Recently, MUPP1 has been shown to be robustly up-regulated by hypertonicity and to be important in the osmotic stress response in tight junctions of kidney cells (51). Finally, altered MUPP1 expression levels have been shown in mice with high predisposition to alcohol and barbiturate physical dependence and withdrawal (52). Taken together, MUPP1 expression levels appear to be highly regulated in several physiological and pathological situations.

In conclusion, our study extends the previously panoply of known functions of MUPP1 on GPCR physiology. MUPP1 regulates G protein-dependent GPCR signaling by directly stabilizing the receptor-G protein complex, which may explain the previously reported high stability of the MT_1-G_i complex. Future studies will concentrate on the still largely unexplored functions of the other PDZ domains of MUPP1 on GPCR function.

Acknowledgments—We are grateful to R. Javier for kindly providing anti-MUPP1 antibodies and GST-PDZ constructs, A. Mancini for GST-PDZ constructs, M. A. Ayoub for the $G\alpha_{i1}$-91-RLuc construct, and C. Bousquet for the human SSTR2 receptor expression vector.

REFERENCES

1. Schultz, J., Copley, R. R., Doerks, T., Ponting, C. P., Bork, P., and Milpetz, F. (2000) *Nucleic Acids Res.* **28,** 231–234
2. Bockaert, J., Roussignol, G., Becamel, C., Gavarini, S., Joubert, L., Dumuis, A., Fagni, L., and Marin, P. (2004) *Biochem. Soc. Trans.* **32,** 851–855
3. He, J., Bellini, M., Inuzuka, H., Xu, J., Xiong, Y., Yang, X., Castleberry, A. M., and Hall, R. A. (2006) *J. Biol. Chem.* **281,** 2820–2827
4. Chen, Z., Hague, C., Hall, R. A., and Minneman, K. P. (2006) *J. Biol. Chem.* **281,** 12414–12420
5. Balasubramanian, S., Fam, S. R., and Hall, R. A. (2007) *J. Biol. Chem.* **282,** 4162–4171
6. Joubert, L., Hanson, B., Barthet, G., Sebben, M., Claeysen, S., Hong, W., Marin, P., Dumuis, A., and Bockaert, J. (2004) *J. Cell Sci.* **117,** 5367–5379
7. Xiang, Y., Devic, E., and Kobilka, B. (2002) *J. Biol. Chem.* **277,** 33783–33790
8. Xia, Z., Gray, J. A., Compton-Toth, B. A., and Roth, B. L. (2003) *J. Biol. Chem.* **278,** 21901–21908
9. Cao, T. T., Deacon, H. W., Reczek, D., Bretscher, A., and von Zastrow, M. (1999) *Nature* **401,** 286–290
10. Paasche, J. D., Attramadal, T., Kristiansen, K., Oksvold, M. P., Johansen, H. K., Huitfeldt, H. S., Dahl, S. G., and Attramadal, H. (2005) *Mol. Pharmacol.* **67,** 1581–1590
11. Lahuna, O., Quellari, M., Achard, C., Nola, S., Meduri, G., Navarro, C., Vitale, N., Borg, J. P., and Misrahi, M. (2005) *EMBO J.* **24,** 1364–1374
12. Hall, R. A., Premont, R. T., Chow, C. W., Blitzer, J. T., Pitcher, J. A., Claing, A., Stoffel, R. H., Barak, L. S., Shenolikar, S., Weinman, E. J., Grinstein, S., and Lefkowitz, R. J. (1998) *Nature* **392,** 626–630
13. Fam, S. R., Paquet, M., Castleberry, A. M., Oller, H., Lee, C. J., Traynelis, S. F., Smith, Y., Yun, C. C., and Hall, R. A. (2005) *Proc. Natl. Acad. Sci. U. S. A.* **102,** 8042–8047
14. Mahon, M. J., Donowitz, M., Yun, C. C., and Segre, G. V. (2002) *Nature* **417,** 858–861
15. Oh, Y. S., Jo, N. W., Choi, J. W., Kim, H. S., Seo, S. W., Kang, K. O., Hwang, J. I., Heo, K., Kim, S. H., Kim, Y. H., Kim, I. H., Kim, J. H., Banno, Y., Ryu,

[6] J.-L. Guillaume, P. Maurice, A. M. Daulat, and R. Jockers, unpublished data.

S. H., and Suh, P. G. (2004) *Mol. Cell. Biol.* **24,** 5069–5079
16. Hu, L. A., Chen, W., Martin, N. P., Whalen, E. J., Premont, R. T., and Lefkowitz, R. J. (2003) *J. Biol. Chem.* **278,** 26295–26301
17. Jeanneteau, F., Guillin, O., Diaz, J., Griffon, N., and Sokoloff, P. (2004) *Mol. Biol. Cell* **15,** 4926–4937
18. Yao, R., Natsume, Y., and Noda, T. (2004) *Oncogene* **23,** 6023–6030
19. Yamada, T., Ohoka, Y., Kogo, M., and Inagaki, S. (2005) *J. Biol. Chem.* **280,** 19358–19363
20. Fromont-Racine, M., Rain, J. C., and Legrain, P. (1997) *Nat. Genet.* **16,** 277–282
21. Zilberfarb, V., Pietri-Rouxel, F., Jockers, R., Krief, S., Delouis, C., Issad, T., and Strosberg, A. D. (1997) *J. Cell Sci.* **110,** 801–807
22. Barritt, D. S., Pearn, M. T., Zisch, A. H., Lee, S. S., Javier, R. T., Pasquale, E. B., and Stallcup, W. B. (2000) *J. Cell. Biochem.* **79,** 213–224
23. Lee, S. S., Glaunsinger, B., Mantovani, F., Banks, L., and Javier, R. T. (2000) *J. Virol.* **74,** 9680–9693
24. Mancini, A., Koch, A., Stefan, M., Niemann, H., and Tamura, T. (2000) *FEBS Lett.* **482,** 54–58
25. Ayoub, M. A., Couturier, C., Lucas-Meunier, E., Angers, S., Fossier, P., Bouvier, M., and Jockers, R. (2002) *J. Biol. Chem.* **277,** 21522–21528
26. Issafras, H., Angers, S., Bulenger, S., Blanpain, C., Parmentier, M., Labbe-Jullie, C., Bouvier, M., and Marullo, S. (2002) *J. Biol. Chem.* **277,** 34666–34673
27. Bousquet, C., Guillermet-Guibert, J., Saint-Laurent, N., Archer-Lahlou, E., Lopez, F., Fanjul, M., Ferrand, A., Fourmy, D., Pichereaux, C., Monsarrat, B., Pradayrol, L., Esteve, J. P., and Susini, C. (2006) *EMBO J.* **25,** 3943–3954
28. Jockers, R., Issad, T., Zilberfarb, V., de Coppet, P., Marullo, S., and Strosberg, A. D. (1998) *Endocrinology* **139,** 2676–2684
29. Brydon, L., Roka, F., Petit, L., deCoppet, P., Tissot, M., Barrett, P., Morgan, P. J., Nanoff, C., Strosberg, A. D., and Jockers, R. (1999) *Mol. Endocrinol.* **13,** 2025–2038
30. Stricker, N. L., Christopherson, K. S., Yi, B. A., Schatz, P. J., Raab, R. W., Dawes, G., Bassett, D. E. J., and Li, M. (1997) *Nat. Biotechnol.* **15,** 336–342
31. Brydon, L., Petit, L., Delagrange, P., Strosberg, A. D., and Jockers, R. (2001) *Endocrinology* **142,** 4264–4271
32. Ullmer, C., Schmuck, K., Figge, A., and Lubbert, H. (1998) *FEBS Lett.* **424,** 63–68
33. Morgan, P. J., Lawson, W., Davidson, G., and Howell, H. E. (1989) *Neuroendocrinology* **50,** 359–362
34. Sneddon, W. B., Syme, C. A., Bisello, A., Magyar, C. E., Rochdi, M. D., Parent, J. L., Weinman, E. J., Abou-Samra, A. B., and Friedman, P. A. (2003) *J. Biol. Chem.* **278,** 43787–43796
35. Morgan, P., Lawson, W., Davidson, G., and Howell, H. (1989) *J. Mol. Endocrinol.* **3,** R5–R8
36. Roka, F., Brydon, L., Waldhoer, M., Strosberg, A. D., Freissmuth, M., Jockers, R., and Nanoff, C. (1999) *Mol. Pharmacol.* **56,** 1014–1024
37. Ayoub, M. A., Maurel, D., Binet, V., Fink, M., Prezeau, L., Ansanay, H., and Pin, J. P. (2007) *Mol. Pharmacol.* **71,** 1329–1340
38. Gutkind, J. S. (2000) *Sci. STKE 2000*, RE1
39. Li, Z., Benard, O., and Margolskee, R. F. (2006) *J. Biol. Chem.* **281,** 11066–11073
40. Zhou, Y. W., Oak, S. A., Senogles, S. E., and Jarrett, H. W. (2005) *Am. J. Physiol.* **288,** C377–C388
41. Becamel, C., Figge, A., Poliak, S., Dumuis, A., Peles, E., Bockaert, J., Lubbert, H., and Ullmer, C. (2001) *J. Biol. Chem.* **276,** 12794–12982
42. Parker, L. L., Backstrom, J. R., Sanders-Bush, E., and Shieh, B. H. (2003) *J. Biol. Chem.* **278,** 21576–21583
43. Stiffler, M. A., Chen, J. R., Grantcharova, V. P., Lei, Y., Fuchs, D., Allen, J. E., Zaslavskaia, L. A., and MacBeath, G. (2007) *Science* **317,** 364–369
44. Gavarini, S., Becamel, C., Altier, C., Lory, P., Poncet, J., Wijnholds, J., Bockaert, J., and Marin, P. (2006) *Mol. Biol. Cell* **17,** 4619–4631
45. Sitek, B., Poschmann, G., Schmidtke, K., Ullmer, C., Maskri, L., Andriske, M., Stichel, C. C., Zhu, X. R., and Luebbert, H. (2003) *Brain Res.* **970,** 178–187
46. Nguyen, M. L., Nguyen, M. M., Lee, D., Griep, A. E., and Lambert, P. F. (2003) *J. Virol.* **77,** 6957–6964
47. Massimi, P., Gammoh, N., Thomas, M., and Banks, L. (2004) *Oncogene* **23,** 8033–8039
48. Latorre, I. J., Roh, M. H., Frese, K. K., Weiss, R. S., Margolis, B., and Javier, R. T. (2005) *J. Cell Sci.* **118,** 4283–4293
49. Slominski, A., Wortsman, J., and Tobin, D. J. (2005) *FASEB J.* **19,** 176–194
50. Dillon, D. C., Easley, S. E., Asch, B. B., Cheney, R. T., Brydon, L., Jockers, R., Winston, J. S., Brooks, J. S., Hurd, T., and Asch, H. L. (2002) *Am. J. Clin. Pathol.* **118,** 451–458
51. Lanaspa, M. A., Almeida, N. E., Andres-Hernando, A., Rivard, C. J., Capasso, J. M., and Berl, T. (2007) *Proc. Natl. Acad. Sci. U. S. A.* **104,** 13672–13677
52. Shirley, R. L., Walter, N. A., Reilly, M. T., Fehr, C., and Buck, K. J. (2004) *Nat. Neurosci.* **7,** 699–700
53. Jelené, F., Oleksy, A., Smietana, K., and Otlewski, J. (2003) *Acta Biochim. Pol.* **50,** 985–1017
54. Pfleger, K. D., and Eidne, K. A. (2006) *Nature Methods* **3,** 165–174
55. Kimber, W. A., Trinkle-Mulcahy, L., Cheung, P. C., Deak, M., Marsden, L. J., Kieloch, A., Watt, S., Javier, R. T., Gray, A., Downes, C. P., Lucocq, J. M., and Alessi, D. R. (2002) *Biochem. J.* **361,** 525–536
56. Hamazaki, Y., Itoh, M., Sasaki, H., Furuse, M., and Tsukita, S. (2003) *J. Biol. Chem.* **277,** 455–461